Amine-Assisted Delamination of Nb_2C MXene for Li-Ion Energy Storage Devices

*Olha Mashtalir, Maria R. Lukatskaya, Meng-Qiang Zhao, Michel W. Barsoum, and Yury Gogotsi**

A new family of 2D materials, known as MXenes, was discovered in 2011.[1] Those are stacks of 2D early transition metal carbides and carbonitrides of general formula $M_{n+1}X_nT_x$, where M stands for metal atom, X stands for C and/or N, n = 1, 2, or 3, and T_x represents various surface terminations (OH, O, and/or F groups). So far, synthesis of nine MXenes of different chemistries has been reported.[2] MXenes exhibit both hydrophilic behavior and metallic conductivity, coupled with good mechanical properties.[3] They are also predicted to show no, or small band gaps, and, depending on their surface termination, should also exhibit magnetic behavior.[4] Such unique combination of properties, which can be further tuned by controlling their compositions and surface chemistries, has attracted much interest in the MXene family of materials as evidenced by an exponentially increasing number of both theoretical and experimental studies on their properties and potential applications.[2]

Energy storage applications, such as batteries[5] and supercapacitors,[6] have attracted most attention so far. These studies have revealed that both, "M" chemistry, and "*n*" number of layers, as well as material and electrode structure affect the performance: (i) M_2X structures show higher Li-ion specific capacities, compared to their M_3X_2 and M_4X_3 counterparts, for the simple reason that the number of atomic layers per MXene sheet in the former are 3 instead of 5 or 7 for the latter;[2,5b] (ii) experimental Li-ion specific capacities of Ti_2CT_x are less than Nb_2CT_x and V_2CT_x;[7] (iii) delaminated MXenes can store more charge than their multilayer counterparts;[6b,8] (iv) introduction of carbon additives, such as carbon nanotubes (CNTs) into the electrode structure improves ion accessibility to the MXene layers and boosts both specific capacities and resulting rate performances.[9]

So far only $Ti_3C_2T_x$ has been synthesized and tested in delaminated form.[6b] To delaminate the latter dimethyl sulfoxide, DMSO, was used. For reasons that are not entirely clear DMSO was not effective in delaminating other MXenes. Electrochemical testing of delaminated $Ti_3C_2T_x$ in Li-ion batteries and supercapacitors showed up to four times improved Li-ion capacities and volumetric capacitances compared to their multilayered counterparts.[6b] Therefore, just like other 2D materials,[10] the importance of developing soft chemical approaches to delaminate other MXenes is crucial to their ultimate use in most applications.

In this Communication, our main goal is to report on the delamination of a second representative of the MXene family –Nb_2CT_x using an amine instead of DMSO. We also show that, not surprisingly, the electrochemical behavior of delaminated Nb_2CT_x/CNT composite electrodes in Li-ion batteries and supercapacitors are superior to their multilayered counterparts.

A schematic illustration of the delamination strategy is depicted in **Figure 1**. It is a two-step process, commonly used to separate a variety of layered materials into 2D sheets,[10] that involves intercalation of an organic compound into the layered structure followed by sonication in a proper solvent. As mentioned above, such a procedure, involving DMSO as an intercalant,[6b] was previously used to delaminate multilayered $Ti_3C_2T_x$ flakes. Since then we showed that delamination of this same compound can also be carried out by simply etching the precursor MAX phase, Ti_3AlC_2, in a solution of a Li salt and an acid, such as LiF and HCl.[6a] Unfortunately, to date, neither of these approaches has been capable of delaminating other MXenes. Therefore, other intercalants had to be considered.

Previously, we have shown that, like some layered transition metal oxides,[11] the Nb_2CT_x surfaces are hydrophilic and terminated mostly with OH groups.[7] Following the analogy with HF etched $Ti_3C_2T_x$, which is negatively charged at the surface, Nb_2CT_x (produced by the same method and carrying the same functional groups) is expected to have acidic behavior and interact with bases and positively charged species.[6b,12] Of particular interest to this work is the delamination of layered niobates using alkylamines and tetraalkylammonium salts.[13] Herein, isopropylamine (i-PrA) was chosen for the following reasons: (i) it forms an ammonium cation $R\text{-}NH_3^+$ when mixed with water, and, thus, can potentially intercalate in-between Nb_2CT_x layers with the assistance of electrostatic forces; (ii) the i-PrA molecule has a three-carbon-atom alkyl tail that is presumably small enough to overcome the steric hindrance upon intercalation and, simultaneously, large enough to push the MXene layers apart leading to weakened interlayer interactions and concomitant delamination.

X-ray diffraction (XRD) patterns of Nb_2CT_x (**Figure 2**a) show in a large shift of the most intense (0002) Nb_2CT_x peak toward lower 2θ angles after exposure to i-PrA. Using this peak position, the *c* lattice parameter (*c*-LP) was found to increase from an initial value of 20.8 Å before amine treatment to 45.4 Å after treatment. The interlayer distance thus increases by ≈12.3 Å, which is large enough to accommodate more than one i-PrA layer and/or water molecules between the Nb_2CT_x layers. It is thus reasonable to assume that due to hydrogen bonding or electrostatic interactions, the i-PrA molecules occupying the

O. Mashtalir, M. R. Lukatskaya, Dr. M.-Q. Zhao, Prof. M. W. Barsoum, Prof. Y. Gogotsi
Department of Materials Science and Engineering and A. J. Drexel Nanomaterials Institute
Drexel University
3141 Chestnut Street, Philadelphia, PA 19104, USA
E-mail: gogotsi@drexel.edu

DOI: 10.1002/adma.201500604

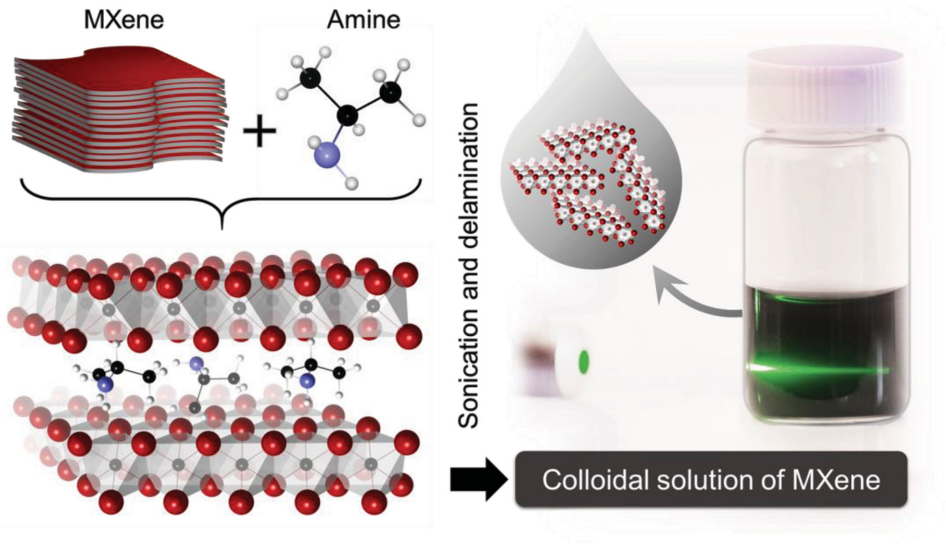

Figure 1. Schematic of Nb_2CT_x delamination process via isopropylamine intercalation. The photo on the right shows Tyndall scattering effect in a colloidal solution of *d*-Nb_2CT_x flakes. In the schematic, the blue spheres represent nitrogen atoms; red represents niobium; black represents carbon; and white represents hydrogen. MXene's surface terminations are not shown.

interlayer space orient themselves with the NH_2 or protonated NH_3^+ end pointing toward the Nb_2CT_x layers and the alkyl part away from the surface.[14] It is also possible that, similar to clays, the amines interact mostly with the acidic edges of the MXene layers wedging the structure open thus allowing water molecules to enter between the layers causing further expansion.[15] The latter can also explain the low content of nitrogen detected by X-ray photoelectron spectroscopy (XPS) (see below). Clearly, more work is needed to understand the exact mechanisms. What the XRD results do unambiguously show, however, is that i-PrA affects all Nb_2CT_x layers equally, as evidenced by the complete disappearance of the peak at 8.4° 2θ.

The presence of nitrogen in the Nb_2CT_x structure, after immersing in i-PrA, was confirmed by XPS. Figure S1b (Supporting Information) clearly shows a weak peak at 401.7 eV that can be attributed to R-NH_3^+.[16] No other pronounced peaks, that could evidence the formation of covalent bonding between the Nb_2CT_x surface and the intercalant amino groups, were observed at lower binding energies in the N region. It follows that the main driving force for amine intercalation into Nb_2CT_x is electrostatic rather than an acid–base reaction as has been reported for layered oxides.[13] It is important to note that since no evidence for covalent bonding between i-PrA and the MXene surface was detected, partial amine de-intercalation can occur when the sample is exposed to the high vacuum and high energy X-rays during XPS analysis resulting in the low intensity peaks in the N-region.

Further delamination of multilayers to individual 2D flakes was achieved by mild sonication of the expanded Nb_2CT_x multilayers in deaerated, deionized (DI) water. The latter was used in order to reduce the chances of oxidation of the MXene particles.[12] After removal of the larger particles by centrifugation, a stable black colloidal solution of delaminated Nb_2CT_x flakes was obtained. Its colloidal nature was confirmed by the

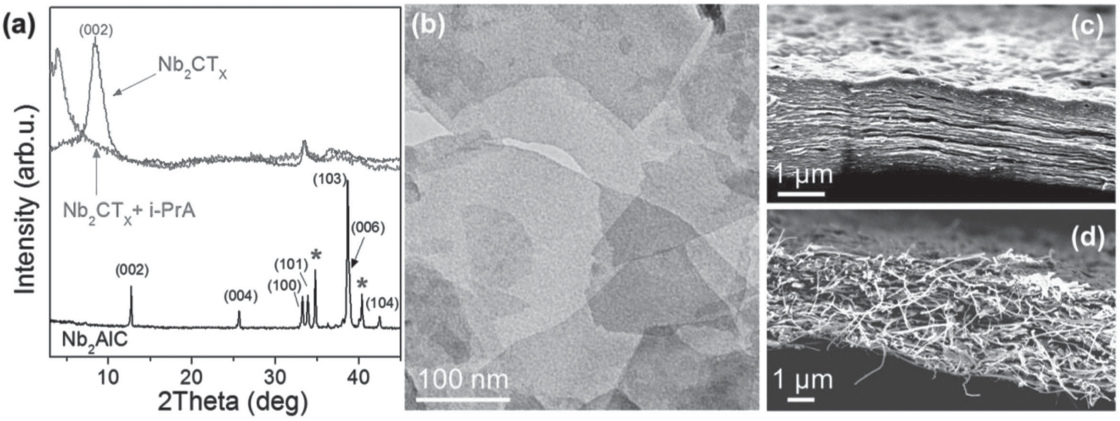

Figure 2. a) XRD patterns of Nb_2AlC powder (bottom), exfoliated Nb_2CT_x, and isopropylamine intercalated Nb_2CT_x (Nb_2CT_x + i-PrA). The peaks denoted by the stars represent NbC peaks that existed in the initial Nb_2AlC as a secondary phase. b) TEM image of the *d*-Nb_2CT_x flakes. Cross-sectional SEM images of c) pure Nb_2CT_x and d) Nb_2CT_x/CNT composite paper.

Tyndall effect, in which, as a result of light scattering, a green light beam is clearly seen when a laser is shined through it (see photo on the right in Figure 1).

When a drop of the colloidal solution was placed on a lacey carbon coated transmission electron microscope (TEM) copper grid and allowed to dry, electron transparent sheets of different sizes, from tens of nanometers up to few micrometers (Figure 2b), were imaged. We anticipate that the flakes' size distribution can be controlled more precisely by choosing proper sonication times and powers, centrifuging times and speeds, etc. Their transparency suggests that the sheets are a few layers thick at most. Similar to graphene,[17] a substantial fraction of the sheets (≈30%) were found to be folded and curved at their edges, evidencing their flexibility (see Figure S2a,b, Supporting Information). The selected area diffraction pattern (inset in Figure S2a, Supporting Information) shows that the flakes maintain the hexagonal symmetry of the parent MAX phase after delamination. The *a* lattice parameter, calculated using the (100) and (110) *d*-spacings from the SAED pattern, was found to be 3.13 Å, which is in excellent agreement with the value reported for its Nb_2AlC precursor, viz., 3.10 Å.[18]

Similar to delaminated $Ti_3C_2T_x$,[6b] the colloidal Nb_2CT_x solution was filtered to create freestanding and flexible paper (Figure 2c). However, we have previously shown that the compact restacking of the MXene flakes, as evidenced herein in Figure 2c, limits electrolyte accessibility to the entire MXene surface and thus reduces the specific capacities and the rates at which the electrodes can be charged and discharged.[9] Said otherwise, if the delaminated flakes are not prevented from restacking, their electrochemical response is even worse than their multilayered counterparts.

It is for this reason that herein, ≈10 wt% CNTs were utilized as interlayer spacers[9,19] that resulted in a more open structure (Figure 2d). To fabricate our electrodes, a CNT dispersion was mixed with the delaminated Nb_2CT_x solution, stirred, and filtered through a polypropylene membrane. The resulting Nb_2CT_x/CNT nanocomposite paper was directly employed as a Li-ion battery electrode in coin cells (against Li foil).

The cyclic voltammetry (CV) profiles of Nb_2CT_x/CNT electrodes look quite similar to the ones reported for multilayer Nb_2CT_x particles,[7] in that no obvious lithiation and delithiation peaks were observed and most of the capacity was generated below 2 V with respect to Li/Li^+ (**Figure 3**a and Figure S3, Supporting Information). At 0.5 C, the Nb_2CT_x/CNT paper yielded a first-cycle capacity of ≈780 mAh g^{-1} and a reversible capacity of ≈420 mAh g^{-1}, with a Coulombic efficiency close to 100% (Figure 3b). The first-cycle irreversibility is most probably caused by the formation of a solid–electrolyte interphase (SEI) layer[20] and possibly an irreversible reaction between Li ions and the surface functional groups on the Nb_2CT_x flakes.[5d] Note that the contribution of CNTs to the overall capacity of the composite paper is negligible due to their limited specific capacity and low mass content.[21]

Upon cycling, the capacity exhibited excellent stability and gradually increased. For instance, the reversible capacity at 2.5 C increased from an initial value of ≈320 to ≈370 mAh g^{-1} after 100 cycles, and to ≈430 mAh g^{-1} after 300 cycles (Figure 3b and Figure S4, Supporting Information). This slow increase

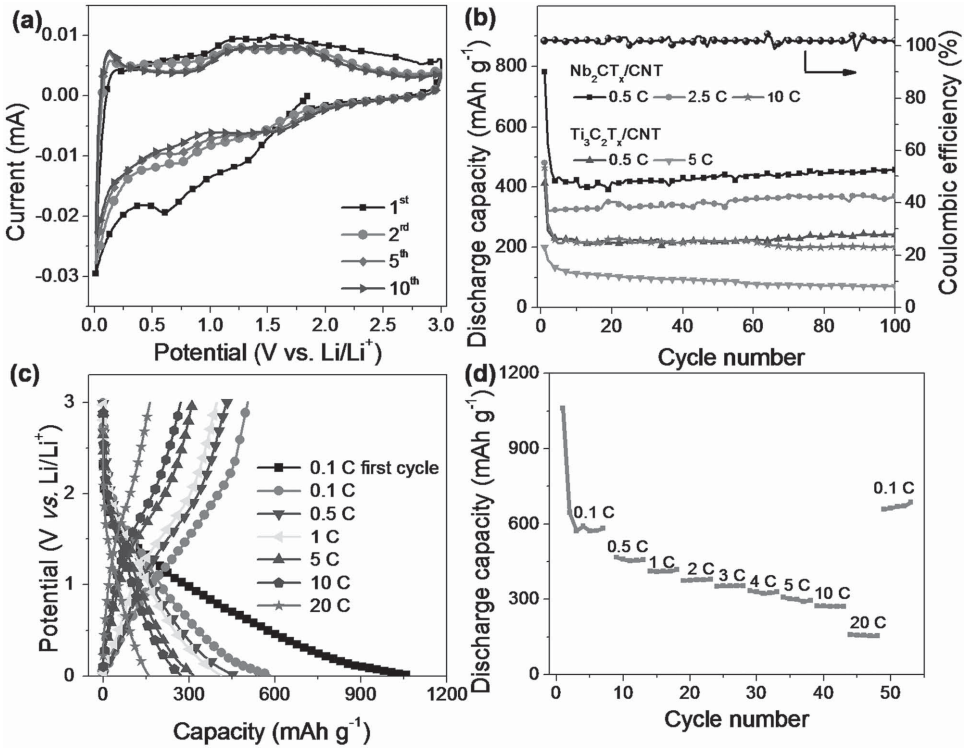

Figure 3. a) CV curves of Nb_2CT_x/CNT paper electrode at a scanning rate of 0.2 mV s^{-1}; b) cycling stability of the Nb_2CT_x/CNT and $Ti_3C_2T_x$/CNT paper electrodes at different cycling rates; c) charge–discharge profiles; and d) discharge capacities of the Nb_2CT_x/CNT electrode at different cycling rates.

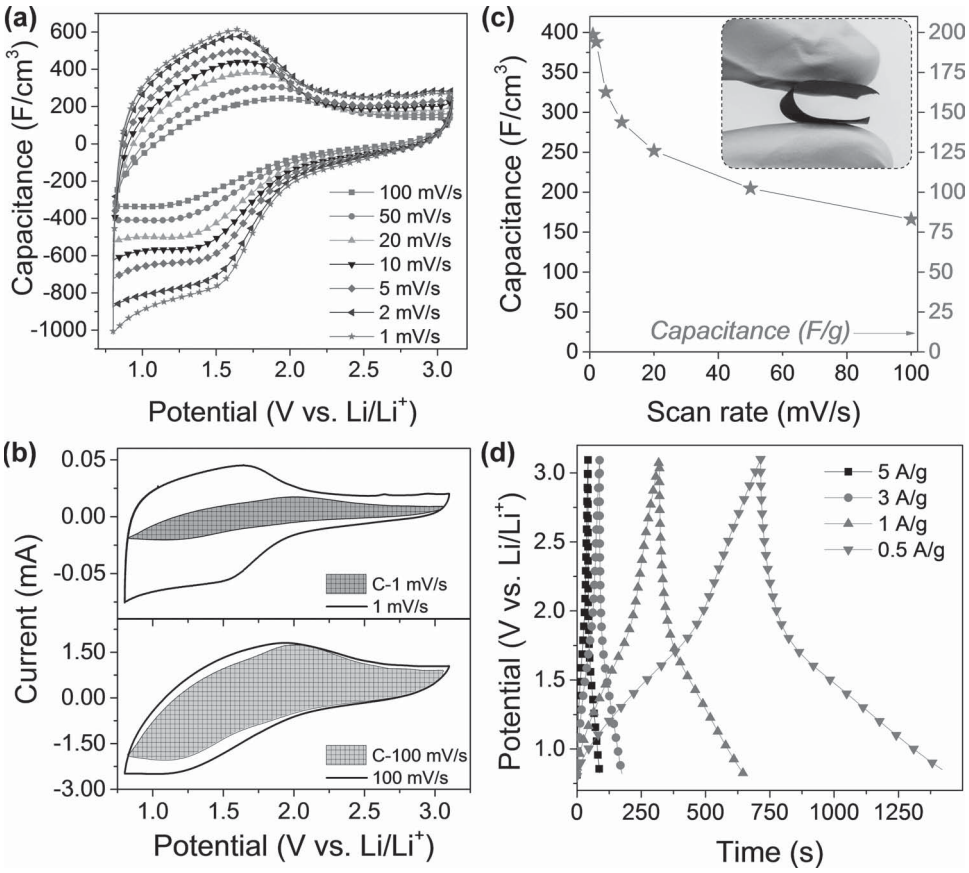

Figure 4. Li-ion capacitor performance of Nb_2CT_x/CNT paper electrodes. a) Cyclic voltammograms at different scan rates and b) cyclic voltammetry profiles collected at 1 and 100 mV s^{-1}. The nonshaded portions represent diffusional capacity; the shaded portions represent the capacitive ("C-") component; c) volumetric (left *y*-axis) and gravimetric (right *y*-axis) rate performances; d) galvanostatic charge–discharge profiles collected at different current densities.

in capacity can be attributed to a gradually improved Li-ion accessibility to active sites as a result of cycling. This slow enhancement with cycling is important because it implies that the values reported here—while quite respectable, especially at high rates—can be further improved with better electrode design/architecture.

Similar to delaminated $Ti_3C_2T_x$,[6b] the capacities obtained for the Nb_2CT_x/CNT paper were larger than those obtained from multilayer Nb_2CT_x particles.[7] However, in good agreement with previous theoretical and experimental results, the values obtained here are higher than those obtained for $Ti_3C_2T_x$/CNT paper with a similar structure (Figure 3c).[5b,7,22]

The Nb_2CT_x/CNT paper electrodes exhibited good specific capacities even at high rates (Figure 3c,d). The first-cycle and reversible capacities obtained at 0.1 C were ≈1060 and ≈600 mAh g^{-1}, respectively. With increasing cycling rates, the capacity decreases, but gradually. Capacities of ≈270 mAh g^{-1} at 10 C and ≈160 mAh g^{-1} at 20 C were obtained. These values are higher than those for lithium titanate at comparable cycling rates.[23]

While the battery performance is promising in terms of capacity, cyclability, and high rate performance, the almost linear charge–discharge profiles (Figure 3c) suggest that Nb_2CT_x behaves electrochemically more like a supercapacitor than a battery.[24] Therefore, we tested it in a Li-ion capacitor configuration against an overcapacitive porous carbon electrode. In **Figure 4**a, CV results are plotted at different scan rates. The overall shape of the CV plots, with a broad peak around 1.5 V versus Li/Li$^+$, resembles that of orthorhombic Nb_2O_5 for which high-rate Li$^+$ intercalation capacitances have been reported.[25] This similarity is consistent with the fact that etching of Nb_2AlC results in the formation of predominantly oxygen-terminated MXenes (see XPS data in Figure S1b, Supporting Information). Notably, the delamination process does not lead to additional oxidation of the material but only results in separation of the multilayer stacks to fewer Nb_2CT_x flakes (Figure 2b). To further quantify the capacitive and diffusion limited (intercalation capacitance) contributions to the overall capacitance we followed the approach described in ref.[26] The results are summarized in Figure 4b: at the lower scan rate of 1 mV s^{-1} (top curve in Figure 4b) intercalation capacitance (the nonshaded area) dominates. At 100 mV s^{-1}, the capacitive component dominates.

As typical for low-conductivity organic electrolytes, we observed a gradual decrease in capacitance with increasing scan rates (Figure 4c). At lower rates, the capacitances—both the gravimetric and, in particular, the volumetric ones—are quite respectable. For instance, at a scan rate of 5 mV s^{-1}, the capacitances were 165 F g^{-1} and 325 F cm^{-3}. Similar to $Ti_3C_2T_x$

paper,[6b] the Nb_2CT_x/CNT paper electrodes are highly flexible (inset in Figure 4c) and thus can be potentially used in flexible/wearable and/or structural energy storage devices.

Galvanostatic charge–discharge profiles (Figure 4d) have a general chevron shape, with the bend point around 1.6–1.7 V versus Li/Li^+. Here again, the calculated Coulombic efficiency of the electrochemical storage process is close to 100%. Table S1 (Supporting Information) summarizes the capacitances calculated from galvanostatic charge–discharge profiles obtained at different current densities. A capacitance retention test performed by galvanostatic cycling at 5 A g^{-1} (Figure S5, Supporting Information) showed that after 200 cycles the capacitance decreased by 15%, after which it stabilized. It is worth noting that if the cell was allowed to rest for 2 h, the capacitance returned to its original first cycle value. Possible explanation is lithium-ion deficiency at the electrode/electrolyte interface during fast Li^+ shuffling due to limited electrolyte conductivity (no capacity drop was observed for the first 300 cycles in Li-ion battery testing (Figure S4, Supporting Information)).

Finally, it is important to note that i-PrA also intercalates other MXenes, such as $Ti_3C_2T_x$ and $Nb_4C_3T_x$. The former was partially delaminated even before sonication (Figure S6, Supporting Information). To intercalate the $Nb_4C_3T_x$, longer treatments (up to two weeks) were required to fully expand the structure (Figure S7, Supporting Information). Crucially, $Nb_4C_3T_x$ is the first M_4C_3 MXene that has been intercalated with small organic molecules. This is important because it implies that the thickness, or stiffness, of the MXene layers is not a limiting factor in the delamination process. It also suggests that other M_4C_3 MXenes can be delaminated if the proper intercalant/solvent combination is found.

In conclusion, Nb_2CT_x was delaminated by intercalating isopropylamine between the Nb_2CT_x layers followed by mild sonication in water. This approach appears to be more universal than our previous method that used dimethyl sulfoxide[8] and can be potentially applied to delaminate $Ti_3C_2T_x$, $Nb_4C_3T_x$, and other MXene family members intercalated with this or other amines.

The colloidal solution obtained after delamination was vacuum filtered with a CNT-containing solution to produce freestanding, flexible CNT/MXene composite "paper" electrodes. When the latter was tested as an anode material, excellent cyclability and Li capacities of more than 400 mAh g^{-1} at 0.5 C were observed. These values are significantly better than values obtained on multilayered (i.e., nondelaminated) material. Moreover, Nb_2CT_x/CNT paper electrodes showed high volumetric capacitance of 325 F cm^{-3} when tested in a Li-ion capacitor configuration.

Experimental Section

Delamination of Nb_2CT_x: To obtain a solution of delaminated Nb_2CT_x sheets, freshly synthesized multilayered Nb_2CT_x (see synthesis details in the Experimental Section in the Supporting Information and in ref.[7] was first intercalated with i-PrA (≥99.5%, Sigma Aldrich, St. Louis, MO) by immersing 1 g of MXene in 10 mL of i-PrA aqueous solution diluted with DI water in a ratio of i-PrA:H_2O as 1:4. After stirring with a magnetic stirrer for 18 h at room temperature (RT), the suspension was centrifuged at 3500 rpm for 10 min and decanted. The remaining intercalated Nb_2CT_x powder was suspended in 250 mL of deaerated DI water and sonicated for 1 h under Ar to prevent oxidation. After sonication, the suspension was centrifuged at 1500 rpm for 1 h and then decanted to separate the colloidal MXene solution from MXene particles that did not delaminate and settled down instead.

To find the concentration of the resulting suspension of delaminated Nb_2CT_x sheets, a certain amount of liquid was filtered through a 0.1 μm pore size filter. The resulting paper was dried in a desiccator, detached from the filter, and weighed. The concentration was found as a ratio of measured mass of delaminated Nb_2CT_x paper to the volume of filtrated liquid, in mg mL^{-1}.

Manufacturing of MXene/CNT Paper: Multiwalled CNTs, prepared through a floating catalyst chemical vapor deposition method,[27] were dispersed in deionized water by sonication for 30 min with the assistance of 0.03 mol L^{-1} sodium dodecylsulphate (99.5%, Fisher Scientific, Fair Lawn, NJ). The CNT dispersion was mixed with the delaminated Nb_2CT_x solution and stirred, and filtered through a polypropylene membrane (3501 Coated PP, Celgard LLC, Charlotte, NC) to yield a composite film. The latter was then dried in air at room temperature and peeled off from the polypropylene membrane, yielding freestanding, flexible Nb_2CT_x/CNT paper. The $Ti_3C_2T_x$/CNT paper was prepared through a similar process starting with a delaminated $Ti_3C_2T_x$ colloidal solution. The concentration of CNTs in these composite papers was controlled at 10 wt%.

Other information on characterization techniques and electrochemical measurements can be found in the Supporting Information.

Supporting Information

Supporting Information is available from the Wiley Online Library or from the author.

Acknowledgements

O.M., M.R.L., and M.-Q.Z. contributed equally to this work. The authors thank Zheng Ling for SEM analysis, Michael Naguib, Michael Ghidiu, Babak Anasori, and Cooper A. Voigt for providing Nb_2AlC and Nb_2CT_x, and Sankalp Kota for help with the electrochemical experiments. The authors thank the Centralized Research Facilities of Drexel University for providing access to XRD, XPS, SEM, and TEM. The battery work was supported by the Assistant Secretary for Energy Efficiency and Renewable Energy, Office of Vehicle Technologies of the U.S. Department of Energy under Contract No. DE-AC02–05CH11231, Subcontract No. 6951370, under the Batteries for Advanced Transportation Technologies (BATT) Program. The Li-ion capacitors work was supported by the Office of Electricity Delivery and Energy Reliability, Energy Storage Systems Program, through Sandia National Laboratories.

Received: February 4, 2015
Revised: March 25, 2015
Published online: April 30, 2015

[1] M. Naguib, M. Kurtoglu, V. Presser, J. Lu, J. J. Niu, M. Heon, L. Hultman, Y. Gogotsi, M. W. Barsoum, *Adv. Mater.* **2011**, *23*, 4248.
[2] M. Naguib, V. N. Mochalin, M. W. Barsoum, Y. Gogotsi, *Adv. Mater.* **2014**, *26*, 992.
[3] a) M. Naguib, O. Mashtalir, J. Carle, V. Presser, J. Lu, L. Hultman, Y. Gogotsi, M. W. Barsoum, *ACS Nano* **2012**, *6*, 1322; b) J. Halim, M. R. Lukatskaya, K. M. Cook, J. Lu, C. R. Smith, L. A. Naslund, S. J. May, L. Hultman, Y. Gogotsi, P. Eklund, M. W. Barsoum, *Chem. Mater.* **2014**, *26*, 2374; c) M. Kurtoglu, M. Naguib, Y. Gogotsi, M. W. Barsoum, *MRS Commun.* **2012**, *2*, 133.

[4] a) M. Khazaei, M. Arai, T. Sasaki, C.-Y. Chung, N. S. Venkataramanan, M. Estili, Y. Sakka, Y. Kawazoe, *Adv. Funct. Mater.* **2013**, *23*, 2185; b) S. Zhao, W. Kang, J. Xue, *Appl. Phys. Lett.* **2014**, *104*, 113106.
[5] a) D. Er, J. Li, M. Naguib, Y. Gogotsi, V. B. Shenoy, *ACS Appl. Mater. Interfaces* **2014**, *6*, 11173; b) Y. Xie, Y. Dall'Agnese, M. Naguib, Y. Gogotsi, M. W. Barsoum, H. L. Zhuang, P. R. C. Kent, *ACS Nano* **2014**, *8*, 9606; c) M. Naguib, J. Come, B. Dyatkin, V. Presser, P.-L. Taberna, P. Simon, M. W. Barsoum, Y. Gogotsi, *Electrochem. Commun.* **2012**, *16*, 61; d) Q. Tang, Z. Zhou, P. Shen, *J. Am. Chem. Soc.* **2012**, *134*, 16909.
[6] a) M. Ghidiu, M. R. Lukatskaya, M.-Q. Zhao, Y. Gogotsi, M. W. Barsoum, *Nature* **2014**, *516*, 78; b) M. R. Lukatskaya, O. Mashtalir, C. E. Ren, Y. Dall'Agnese, P. Rozier, P. L. Taberna, M. Naguib, P. Simon, M. W. Barsoum, Y. Gogotsi, *Science* **2013**, *341*, 1502.
[7] M. Naguib, J. Halim, J. Lu, K. M. Cook, L. Hultman, Y. Gogotsi, M. W. Barsoum, *J. Am. Chem. Soc.* **2013**, *135*, 15966.
[8] O. Mashtalir, M. Naguib, V. N. Mochalin, Y. Dall'Agnese, M. Heon, M. W. Barsoum, Y. Gogotsi, *Nat. Commun.* **2013**, *4*, 1716.
[9] M.-Q. Zhao, C. E. Ren, Z. Ling, M. R. Lukatskaya, C. Zhang, K. L. Van Aken, M. W. Barsoum, Y. Gogotsi, *Adv. Mater.* **2015**, *27*, 339.
[10] a) Q. Tang, Z. Zhou, *Prog. Mater. Sci.* **2013**, *58*, 1244; b) V. Nicolosi, M. Chhowalla, M. G. Kanatzidis, M. S. Strano, J. N. Coleman, *Science* **2013**, *340*, 1226419.
[11] a) R. Ma, T. Sasaki, *Adv. Mater.* **2010**, *22*, 5082; b) M. Osada, T. Sasaki, *J. Mater. Chem.* **2009**, *19*, 2503.
[12] O. Mashtalir, K. M. Cook, V. N. Mochalin, M. Crowe, M. W. Barsoum, Y. Gogotsi, *J. Mater. Chem. A* **2014**, *2*, 14334.
[13] M. A. Bizeto, A. L. Shiguihara, V. R. L. Constantino, *J. Mater. Chem.* **2009**, *19*, 2512.
[14] Y. Komori, Y. Sugahara, K. Kuroda, *Appl. Clay Sci.* **1999**, *15*, 241.
[15] B. Rotenberg, *MRS Bull.* **2014**, *39*, 1074.
[16] O. C. Compton, D. A. Dikin, K. W. Putz, L. C. Brinson, S. T. Nguyen, *Adv. Mater.* **2010**, *22*, 892.
[17] S. Rotkin, Y. Gogotsi, *Mater. Res. Innov.* **2002**, *5*, 191.
[18] M. W. Barsoum, *MAX Phases*, Wiley-VCH, Weinheim, Germany **2013**.
[19] a) S. Li, Y. Luo, W. Lv, W. Yu, S. Wu, P. Hou, Q. Yang, Q. Meng, C. Liu, H.-M. Cheng, *Adv. Energy Mater.* **2011**, *1*, 486; b) H.-J. Peng, J.-Q. Huang, M.-Q. Zhao, Q. Zhang, X.-B. Cheng, X.-Y. Liu, W.-Z. Qian, F. Wei, *Adv. Funct. Mater.* **2014**, *24*, 2772; c) M. Yang, Y. Hou, N. A. Kotov, *Nano Today* **2012**, *7*, 430; d) M.-Q. Zhao, X.-F. Liu, Q. Zhang, G.-L. Tian, J.-Q. Huang, W. Zhu, F. Wei, *ACS Nano* **2012**, *6*, 10759; e) M.-Q. Zhao, Q. Zhang, J.-Q. Huang, G.-L. Tian, J.-Q. Nie, H.-J. Peng, F. Wei, *Nat. Commun.* **2014**, *5*, 3410.
[20] S. J. Kim, M. Naguib, M. Zhao, C. Zhang, H.-T. Jung, M. W. Barsoum, Y. Gogotsi, *Electrochim. Acta* **2015**, *163*, 246.
[21] a) B. J. Landi, M. J. Ganter, C. D. Cress, R. A. DiLeo, R. P. Raffaelle, *Energy Environ. Sci.* **2009**, *2*, 638; b) C. de las Casas, W. Li, *J. Power Sources* **2012**, *208*, 74.
[22] Y. Xie, M. Naguib, V. N. Mochalin, M. W. Barsoum, Y. Gogotsi, X. Yu, K. W. Nam, X. Q. Yang, A. I. Kolesnikov, P. R. Kent, *J. Am. Chem. Soc.* **2014**, *136*, 6385.
[23] a) J. Liu, J. S. Chen, X. Wei, X. W. Lou, X.-W. Liu, *Adv. Mater.* **2011**, *23*, 998; b) Y. Tang, L. Yang, Z. Qiu, J. Huang, *J. Mater. Chem.* **2009**, *19*, 5980.
[24] P. Simon, Y. Gogotsi, B. Dunn, *Science* **2014**, *343*, 1210.
[25] V. Augustyn, J. Come, M. A. Lowe, J. W. Kim, P.-L. Taberna, S. H. Tolbert, H. D. Abruña, P. Simon, B. Dunn, *Nat. Mater.* **2013**, *12*, 518.
[26] J. Wang, J. Polleux, J. Lim, B. Dunn, *J. Phys. Chem. C* **2007**, *111*, 14925.
[27] Q. Zhang, J.-Q. Huang, M.-Q. Zhao, W.-Z. Qian, Y. Wang, F. Wei, *Carbon* **2008**, *46*, 1152.